International Journal of Astronomy and Astrophysics, 2026, 16(3), 254-272
https://www.scirp.org/journal/ijaa
ISSN Online: 2161-4725
ISSN Print: 2161-4717

# Transport in Astrophysics: X. The Integral of the Planck Distribution

**Lorenzo Zaninetti**

Physics Department, University of Turin, Turin, Italy
Email: l.zaninetti@alice.it

**How to cite this paper:** Zaninetti, L. (2026) Transport in Astrophysics: X. The Integral of the Planck Distribution. *International Journal of Astronomy and Astrophysics*, **16**, 254-272.
https://doi.org/10.4236/ijaa.2026.163016

**Received:** June 30, 2026
**Accepted:** August 29, 2026
**Published:** September 1, 2026



## Abstract

The integral of the Planck distribution for radiation in the wavelength version can be integrated in terms of polylogarithms. We can therefore introduce a theoretical color theory for astronomical purposes. In particular, we investigate the two colors (B-V) and (U-B) and the bolometric correction in the framework of the incomplete Planck integral. Some of the astronomical variables of the Hertzsprung-Russel diagram, such as the absolute visual magnitude, radius, and mass, are derived as functions of (B-V) for nearby main sequence stars. The logarithm of the gravity is derived as a function of the temperature.

## Keywords

Stars: Atmospheres, Radiation Mechanisms: General, Blackbody Radiation

## 1. Introduction

We start with a brief review of the integration of the blackbody distribution in terms of frequency or wavelength. The first analytical expression in terms of polylogarithms for the fractional emissive power of a blackbody spectral distribution in any wavelength was found in 1981 by [1], followed by [2]-[7]. The entropy of the radiation distribution from a statistical perspective was derived in [8]. A modern analysis of the evaluation of the integral of the Planck blackbody function over a finite spectral range can be found in [9]. We now outline some approaches to the color systems in stars. The color (B-V) was carefully analyzed by [10] in terms of temperature, $T_{eff}$, $(B\text{-}V)_0$, [Fe/H] and $\log(g)$. The color-color diagram has been deduced in the framework of Planck's general law, see [11]. We now pose some questions which have not yet been analyzed.

1. Is it possible to evaluate the integral of the spectral radiance for the Planck distribution in terms of frequencies or wavelengths?

2. Can the astronomical colors, such as (B-V) or (U-B), and the bolometric cor-

rection, be modeled by the analytical integral of the Planck distribution?

3. Can we model the variables of the Hertzsprung-Russell diagram, such as the temperature, mass, radius, visual magnitude, luminosity and gravity, in the newly developed framework?

In order to answer the above questions, Section 2 analyzes a pseudo-monochromatic color system which can be considered a standard reference, and then Section 3 introduces the polylogarithms, evaluates the integral of the incomplete Planck distribution, applies the integral to the evaluation of the color (B-V) and derives the bolometric correction in the new framework. An update to the theoretical Hertzsprung-Russell diagram is carried out in Section 4 in agreement with the new results.

## 2. The Color System

The spectral radiance of the Planck distribution as a function of the wavelength, $\lambda$, is

$$B_\lambda(\lambda,T)=\frac{2hc^2}{\lambda^5\left(\mathrm{e}^{\frac{hc}{\lambda kT}}-1\right)}\ \mathrm{W}\cdot\mathrm{sr}^{-1}\cdot\mathrm{m}^{-3}, \tag{1}$$

see, as an example, equation (3.52) in [12] or formula (2.88) in [4]. The color-difference, $(C_1-C_2)$, can be expressed as

$$(C_1-C_2)=m_1-m_2=K-2.5\log_{10}\frac{\int S_1 I_\lambda \mathrm{d}\lambda}{\int S_2 I_\lambda \mathrm{d}\lambda}, \tag{2}$$

where $m_1$ is the apparent magnitude at color 1, $m_2$ is the apparent magnitude at color 2, $S_\lambda$ is the sensitivity function in the region specified by the index $\lambda$, $K$ is a constant, and $I_\lambda$ is the energy flux reaching the earth. We now define a sensitivity function for a pseudo-monochromatic system

$$S_\lambda=\delta(\lambda-\lambda_i)\quad i=U,B,V,R,I, \tag{3}$$

where $\delta$ denotes the Dirac delta function. In this pseudo-monochromatic color system, the color-difference is

$$(C_1-C_2)=K-2.5\log_{10}\frac{\lambda_2^5}{\lambda_1^5}\frac{\left(\exp\left(\frac{hc}{\lambda_2 kT}\right)-1\right)}{\left(\exp\left(\frac{hc}{\lambda_1 kT}\right)-1\right)}, \tag{4}$$

where the wavelengths $\lambda_1$ and $\lambda_2$ are those of colors $C_1$ and $C_2$. **Table 1** presents the central value in nm of the considered band and the full width at half maximum (FWHM) of the considered color.

**Table 1.** Photometric system.

| symbol | wavelength (nm) | FWHM (nm) |
|---|---|---|
| $U$ | 365 | 66 |
| $B$ | 445 | 94 |

**Continued**

| | | |
|---|---|---|
| $V$ | 551 | 88 |
| $R$ | 658 | 138 |
| $I$ | 806 | 149 |

The previous expression for the color can be expanded in a Taylor series about the point $T=\infty$. When the order of the expansion is 2, we have

$$(C_1-C_2)_{app}=-\frac{5\ln\left(\frac{\lambda_2^4}{\lambda_1^4}\right)}{2\ln(10)}-\frac{5\left(\frac{hc\lambda_2^3}{2\lambda_1^4k}-\frac{\lambda_2^4hc}{2\lambda_1^5k}\right)\lambda_1^4}{2\lambda_2^4\ln(10)T},\ \text{order 2,} \tag{5}$$

where the index $app$ means approximated. When the order of the expansion is 3,

$$(C_1-C_2)_{app}=\frac{-\frac{5\ln\left(\frac{\lambda_2^4}{\lambda_1^4}\right)T^2k^2\lambda_1^2\lambda_2^2}{2}-\frac{5(\lambda_1-\lambda_2)h\left(\left(Tk\lambda_2+\frac{hc}{12}\right)\lambda_1+\frac{ch\lambda_2}{12}\right)c}{4}}{(\ln(2)+\ln(5))T^2k^2\lambda_1^2\lambda_2^2},\ \text{order 3.} \tag{6}$$

Figure 1 presents the exact definition of (B-V) together with the two Taylor approximations of orders 2 and 3 just derived and the astronomical data for the observed (B-V) as reported in figure 3 in [5]. The three theoretical lines are calibrated in such a way that (B-V) = −0.33 at $T=42000$ K.

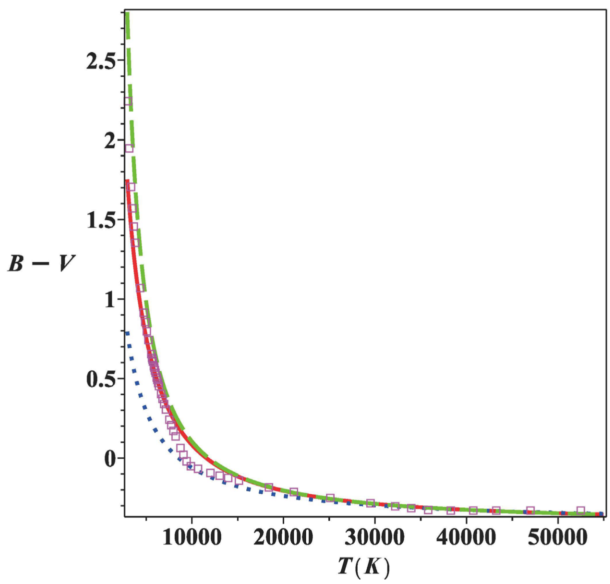


**Figure 1.** Definition of color (B-V) in the pseudo-monochromatic color system with Equation (4), red full line, Taylor expansion of order 2 with Equation (5), blue dotted line, Taylor expansion of order 3 with Equation (6), green dashed line, and (B-V) observed data [5], magenta squares.

Another interesting quantity to be explored is the bolometric correction $BC$, defined as always negative

$$BC = M_{\text{bol}} - M_V, \tag{7}$$

where $M_{\text{bol}}$ is the absolute bolometric magnitude and $M_V$ is the absolute visual magnitude. It can be expressed as

$$BC = \frac{5}{2}\frac{\ln\left(15\left(\frac{hc}{kT\pi}\right)^4\left(\frac{1}{\lambda_V}\right)^5\frac{1}{\exp\left(\frac{hc}{kT\lambda_V}\right)-1}\right)}{\ln(10)} + K_{BC}, \tag{8}$$

where $\lambda_V$ is the visual wavelength and $K_{BC}$ a constant. We now expand $BC$ in a Taylor series of order 3 about the point $T = \infty$

$$\begin{aligned} BC_{app,3} = {} & -\ln\left(\left(\frac{15h^3c^3}{\lambda_1^4k^3\pi^4T^3}\right)^{-\frac{5}{2\ln(10)}}\right) - \frac{5hc}{4k\lambda_1\ln(10)T} \\ & -\frac{5h^2c^2}{48k^2\lambda_1^2\ln(10)T^2} + K_{BC}, \text{ order } 3. \end{aligned} \tag{9}$$

The Taylor series of order 7 about the point $T = \infty$ is

$$\begin{aligned} BC_{app,7} = {} & -\ln\left(\left(\frac{15h^3c^3}{\lambda_1^4k^3\pi^4T^3}\right)^{-\frac{5}{2\ln(10)}}\right) - \frac{5hc}{4k\lambda_1\ln(10)T} - \frac{5h^2c^2}{48k^2\lambda_1^2\ln(10)T^2} \\ & + \frac{h^4c^4}{1152k^4\lambda_1^4\ln(10)T^4} - \frac{h^6c^6}{72576k^6\lambda_1^6\ln(10)T^6} + K_{BC}, \text{ order } 7. \end{aligned} \tag{10}$$

We now summarize three methods which allow finding the temperature, $T_{max}$, that corresponds to the maximum value of the bolometric correction, $BC_{max}$. The first method solves numerically for when the first derivative of the Planck distribution as represented by Equation (1) is zero:

$$\frac{\partial B_\lambda(T)}{\partial T} = 8.35639\times10^{-24}\left(\frac{3.39271\times10^{27}\,\mathrm{e}^{\frac{26112}{T}}}{\left(\mathrm{e}^{\frac{26112}{T}}-1.0\right)^2T^6} - \frac{5.19715\times10^{23}}{\left(\mathrm{e}^{\frac{26112}{T}}-1.0\right)T^5}\right)\left(\mathrm{e}^{\frac{26112}{T}}-1.0\right)T^4 = 0, \tag{11}$$

and the result is

$$T_{max} = 6660.0697\ \text{K}. \tag{12}$$

The second method evaluates the first derivative of the Taylor series of order 3 and sets it equal to zero:

$$\begin{aligned} \frac{\partial B_{app,3}(\lambda_1,T)}{\partial T} = {} & -\frac{15}{2\ln(10)T} + \frac{9.053703309\times10^{22}\,hc}{\lambda_1\ln(10)T^2} \\ & + \frac{1.092927248\times10^{45}\,h^2c^2}{\lambda_1^2\ln(10)T^3} \\ = {} & 0, \end{aligned} \tag{13}$$

which has the positive analytical solution

$$T_{max} = \frac{\left(\frac{\sqrt{5}}{2}+\frac{1}{2}\right)hc}{6k\lambda_1} = 7041.7\ \text{K}. \tag{14}$$

The third method evaluates sets the first derivative of the Taylor series of order 7 equal to zero:

$$\begin{aligned}\frac{\partial B_{app,7}(T)}{\partial T} &= -\frac{7.5}{\ln(10)T}+\frac{32640}{\ln(10)T^2}+\frac{1.4205\times10^8}{\ln(10)T^3} \\ &\quad -\frac{1.61425\times10^{15}}{\ln(10)T^5}+\frac{2.62063\times10^{22}}{\ln(10)T^7} \\ &= 0,\end{aligned} \tag{15}$$

which is an algebraic equation of degree 6. The above equation has four complex solutions, a negative solution, and a positive solution, which is

$$T_{max} = 6717.0477\ \text{K}. \tag{16}$$

The constant $K_{BC}$ can be evaluated by equating the theoretical $BC$ with the observed one.

Figure 2 presents the exact definition of the $BC$ together with the two Taylor approximations of orders 3 and 7 just derived and the astronomical data for the observed $BC$ for the main sequence as reported in table 15.7 in [13].

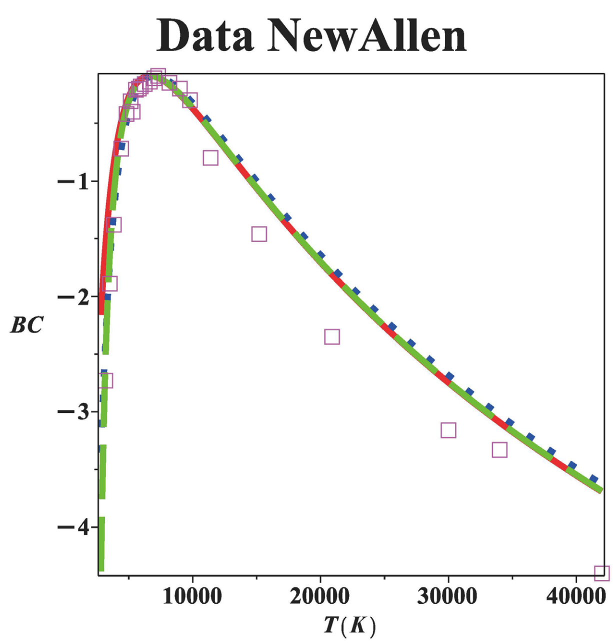


Figure 2. Definition of the bolometric correction ($BC$) with Equation (7), red full line, Taylor expansion of order 3 with Equation (13), blue dotted line, Taylor expansion of order 7 with Equation (15), green dashed line, and $BC$ of observed data, magenta squares.

## 3. The Incomplete Planck Integral

### 3.1. Polylogarithms

The polylogarithms when $z \le 1$ are defined as

$$\mathrm{Li}_a(z)=\sum_{n=1}^{\infty}\frac{z^n}{n^a}\qquad z\le 1 \tag{17}$$

where $z$ and $a$ are complex variables, see [14]. We can evaluate the polylogarithms when $z\ge 1$ through the inversion formula

$$\mathrm{Li}_s(z)=-\frac{\mathrm{Li}_s\left(\frac{1}{z}\right)(-1)^s s!+(2\mathrm{I}\pi)^s B_s\left(\frac{-\frac{\mathrm{I}}{2}\ln(z)}{\pi}\right)}{s!}\qquad z\ge 1, \tag{18}$$

where $B_s$ is the Bernoulli number with index $s$ and $\mathrm{I}$ a square root of -1. A practical implementation of the above formula when $s=2$ is

$$\mathrm{Li}_2(z)=\mathrm{I}\ln(z)\pi-\frac{\ln(z)^2}{2}+\frac{\pi^2}{3}-\mathrm{Li}_2\left(\frac{1}{z}\right)\qquad z\ge 1, \tag{19}$$

when $s=3$, this is

$$\mathrm{Li}_3(z)=\frac{\pi^2\ln(z)}{3}-\frac{\ln(z)^3}{6}+\frac{\mathrm{I}\pi\ln(z)^2}{2}+\mathrm{Li}_3\left(\frac{1}{z}\right)\qquad z\ge 1, \tag{20}$$

when $s=4$, it is

$$\mathrm{Li}_4(z)=\frac{\mathrm{I}\ln(z)^3\pi}{6}+\frac{\pi^4}{45}+\frac{\ln(z)^2\pi^2}{6}-\frac{\ln(z)^4}{24}-\mathrm{Li}_4\left(\frac{1}{z}\right)\qquad z\ge 1. \tag{21}$$

When $z\ge 1$, we can introduce an asymptotic expansion of order 7 when $a$ is 2, 3, or 4:

$$\mathrm{Li}_2(z)=\frac{12\pi^2z^3-36\mathrm{I}\ln(z)\pi z^3-18\ln(z)^2z^3-36z^2-9z-4}{36z^3}\qquad z\ge 1, \tag{22}$$

$$\mathrm{Li}_3(z)=\frac{-36\ln(z)^3z^3-108\mathrm{I}\ln(z)^2\pi z^3+72\ln(z)\pi^2z^3+216z^2+27z+8}{216z^3}\qquad z\ge 1, \tag{23}$$

$$\mathrm{Li}_4(z)=\frac{-270\ln(z)^4z^3-1080\mathrm{I}\ln(z)^3\pi z^3+1080\ln(z)^2\pi^2z^3+144\pi^4z^3-6480z^2-405z-80}{6480z^3}\qquad z\ge 1. \tag{24}$$

In order to visualize these three asymptotic expansions, **Figures 3-5** compare the real part of the polylog and its asymptotic expansion for $a=2$, $a=3$ and $a=4$.

### 3.2. The Integral

The integral of the spectral radiance for the Planck distribution in wavelengths, $F(\lambda,T)$, is

$$F(\lambda,T)=\frac{hc^2}{2\lambda^4}-\frac{2ckT\ln\left(1-\mathrm{e}^{\frac{hc}{\lambda kT}}\right)}{\lambda^3}-\frac{6k^2T^2\mathrm{Li}_2\left(\mathrm{e}^{\frac{hc}{\lambda kT}}\right)}{h\lambda^2}+\frac{12k^3T^3\mathrm{Li}_3\left(\mathrm{e}^{\frac{hc}{\lambda kT}}\right)}{h^2c\lambda}-\frac{12k^4T^4\mathrm{Li}_4\left(\mathrm{e}^{\frac{hc}{\lambda kT}}\right)}{h^3c^2}, \tag{25}$$

where the polylogarithms, $\mathrm{Li}_2,\mathrm{Li}_3$ and $\mathrm{Li}_4$, were defined in the previous subsection. Therefore the spectral radiance, $I(\lambda_{low},\lambda_{upp},T)$, comprised between the lower wavelength, $\lambda_{low}$, and the upper wavelength, $\lambda_{upp}$, is

$$I(\lambda_{low},\lambda_{upp},T)=F(\lambda_{upp},T)-F(\lambda_{low},T). \tag{26}$$

The two values of the wavelength can be found with the following empirical rule

$$\lambda_{low} = \text{considered wavelength} - \text{FWHM}/2, \tag{27a}$$

$$\lambda_{upp} = \text{considered wavelength} + \text{FWHM}/2, \tag{27b}$$

where the considered wavelength and the FWHM are given in Table 1 for the colors here considered. The color-difference in the framework of incomplete Planck integrals is

$$(C_1 - C_2) = K - 2.5\log_{10}(R), \tag{28}$$

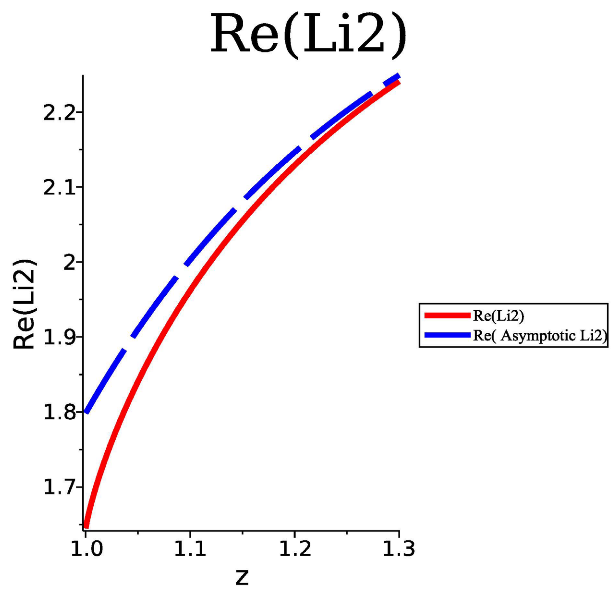


Figure 3. Real part of $\mathrm{Li}_2(z)$, red full line, and real part of the asymptotic $\mathrm{Li}_2(z)$, blue dashed line.

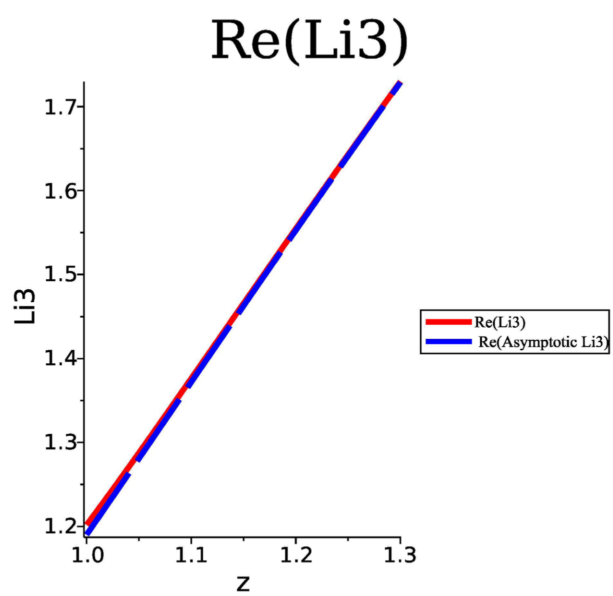


Figure 4. Real part of $\mathrm{Li}_3(z)$, red full line, and real part of the asymptotic $\mathrm{Li}_3(z)$, blue dashed line.

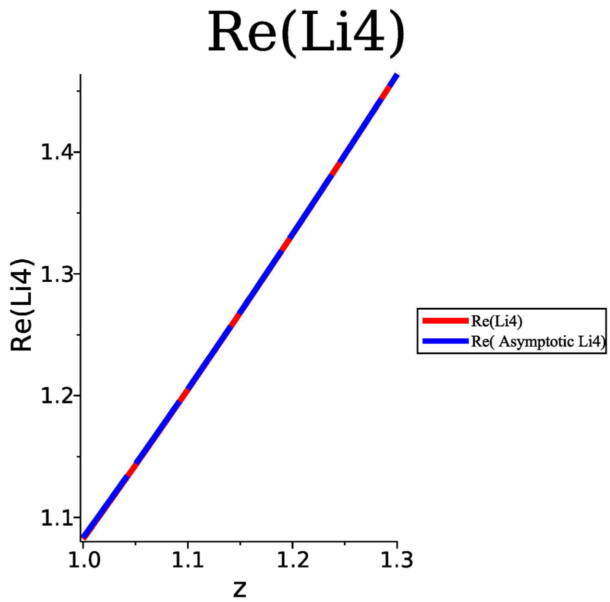


**Figure 5.** Real part of $\mathrm{Li}_4(z)$, red full line, and real part of the asymptotic $\mathrm{Li}_4(z)$, blue dashed line.

where

$$R = \frac{I(\lambda_{1,low}, \lambda_{1,upp}, T)}{I(\lambda_{2,low}, \lambda_{2,upp}, T)}, \tag{29}$$

where the index 1/2 mean colors $C_1/C_2$ and upp/low mean upper/lower.

**Figure 6** presents the color (B-V) as a function of the temperature as given by the incomplete Planck integral.

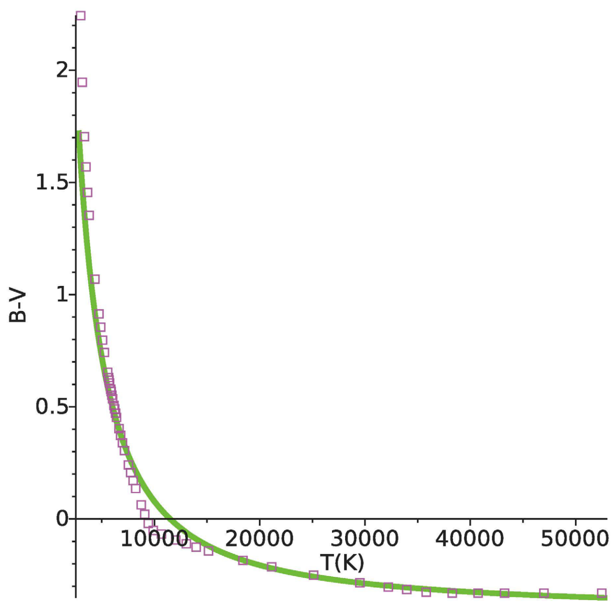


**Figure 6.** (B-V) as a function of the temperature as derived with polylogarithms, green full line, and (B-V) observed data [5], magenta squares; the calibration is (B-V) = −0.33 at $T = 42000$ K.

Another way to present the theoretical colors as derived with polylogarithms is to present the results as a function of $1/T$. This transforms a nearly hyperbolic behavior into a nearly rectilinear behavior, see **Figure 7** for (B-V) and **Figure 8** for (U-B).

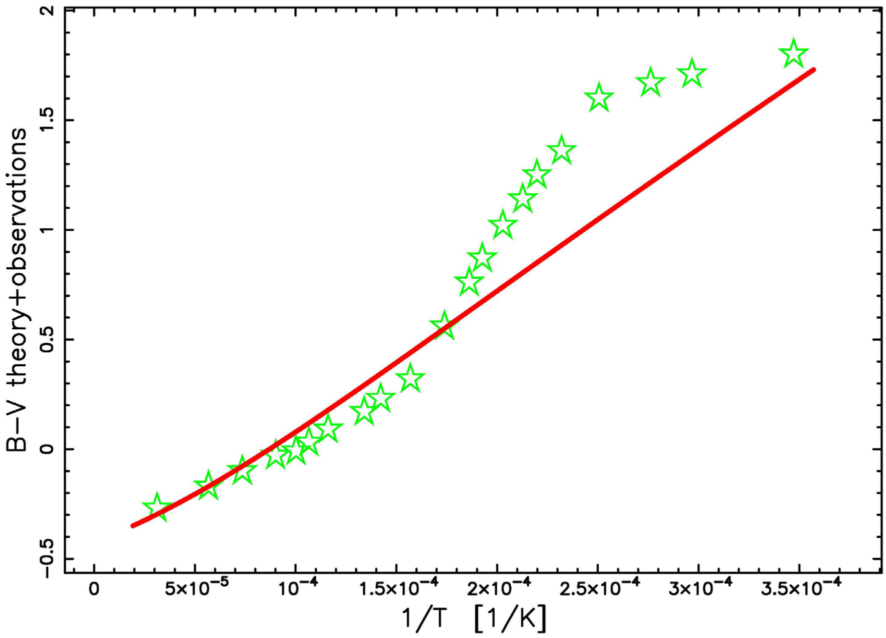


**Figure 7.** (B-V) as derived with polylogarithms versus $1/T$, red line, and (B-V) observed data [5], green stars; the calibration is (B-V) = −0.33 at $T = 42000$ K.

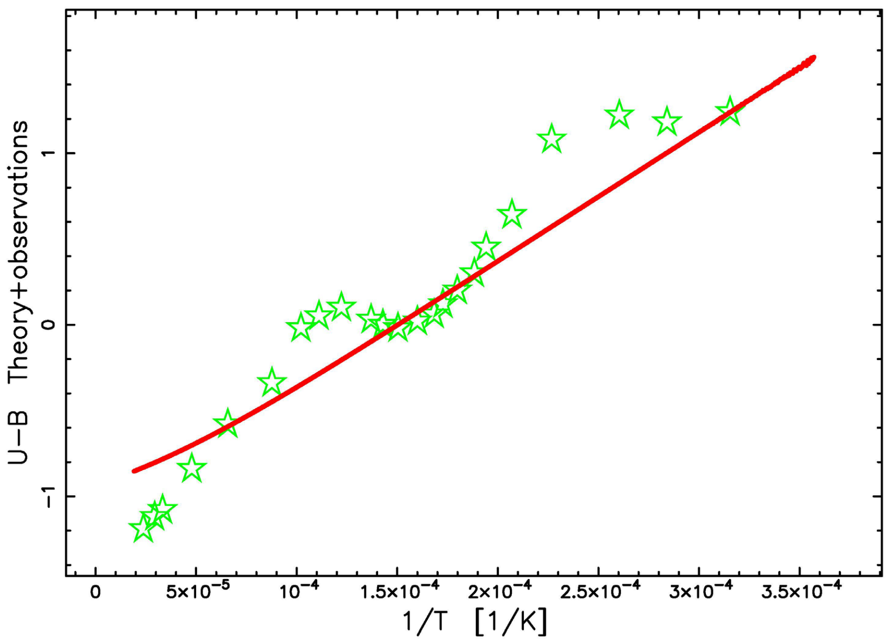


**Figure 8.** (U-B) as derived with polylogarithms versus $1/T$, red line, and (U-B) observed data [13], green stars; the calibration is (U-B) = 1.24 at $T = 3170$ K.

We now continue testing the hypothesis of a nearly rectilinear relation between the theoretical color and the inverse of the temperature with the three approximations

$$(C_1 - C_2) = a + b/T, \tag{30a}$$

$$(C_1 - C_2) = a + b/T + c/T^2, \tag{30b}$$

$$(C_1 - C_2) = \frac{a + b/T + c/T^2}{d + e/T}. \tag{30c}$$

The resulting fits are

$$(C_1 - C_2) = \frac{6326.4183319}{T} - 0.53664796031, \tag{31a}$$

$$(C_1 - C_2) = \frac{1.4460283399 \times 10^6}{T^2} + \frac{5782.6960194}{T} - 0.49935325856, \tag{31b}$$

$$(C_1 - C_2) = \frac{\frac{210524.356319178}{T^2} - \frac{16.5114244569337}{T} - 0.00014538600531}{\frac{32.018248772}{T} + 0.00051834459911}. \tag{31c}$$

The above relations can be inverted in order to find the temperature as a function of the color, for example (B-V):

$$T = \frac{1}{0.000158067(\text{B-V}) + 0.0000848265}, \tag{32a}$$

$$T = \frac{2.6042 \times 10^{19} + 4096.0\sqrt{4.3917 \times 10^{31} + 6.9925 \times 10^{30}(\text{B-V})}}{9.0071 \times 10^{15}(\text{B-V}) + 4.4977 \times 10^{15}}, \tag{32b}$$

$$T = \frac{N}{D}. \tag{32c}$$

where

$$\begin{aligned} N = & -5.90632 \times 10^{20}(\text{B-V}) - 3.04582 \times 10^{20} \\ & + 32768\sqrt{3.24888 \times 10^{32}(\text{B-V})^2 + 4.73413 \times 10^{32}(\text{B-V}) + 1.25198 \times 10^{32}}, \end{aligned} \tag{33}$$

and

$$D = 1.91235 \times 10^{16}(\text{B-V}) + 5.36379 \times 10^{15}. \tag{34}$$

We are now ready to derive the temperature as a function of the observed color (B-V) and a first comparison can be done including also the empirical Olson's fit [15], which is

$$T = 1000 + \frac{5000}{(\text{B-V}) + 0.5}, \tag{35}$$

see **Figure 9**.

A second comparison can be done with the Ballesteros fit, see Equation (14) in [11], which is

$$T = \frac{4600}{0.92(\text{B-V}) + 1.7} + \frac{4600}{0.92(\text{B-V}) + 0.62}, \tag{36}$$

see Figure 10.

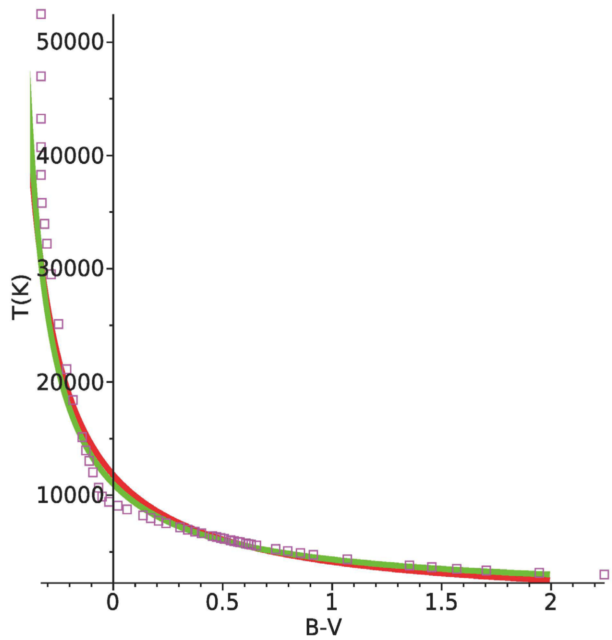


Figure 9. $T$ as a function of (B-V) as in Equation (32a), red line, Olson's fit, green line, and observed data [5], purple squares.

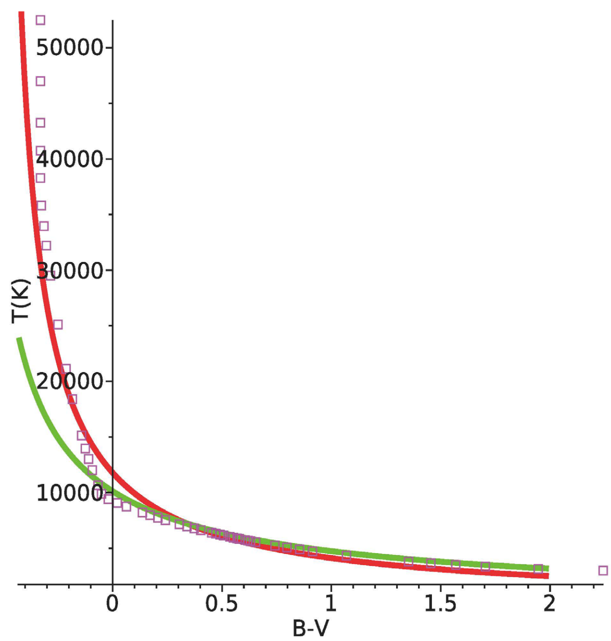


Figure 10. $T$ as a function of (B-V) as in Equation (32a), red line, Ballesteros's fit, green line, and observed data [5], purple squares.

### 3.3. The Bolometric Correction

The bolometric correction has been defined by Equation (7) and in the case of the integral with polylogarithms is calibrated in such a way that $BC = -0.09$ at $T = 6690$ K:

$$\begin{aligned}BC = 352.503 + 1.08573\ln\Bigg(\Bigg|&7.22180\times10^{-141}\,\mathrm{Li}_{4.0}\left(\mathrm{e}^{\frac{24181}{T}}\right)T^4\\&-7.2218\times10^{-141}\,\mathrm{Li}_{4.0}\left(\mathrm{e}^{\frac{28378.2}{T}}\right)T^4 - 1.7463\times10^{-136}\,\mathrm{Li}_{3.0}\left(\mathrm{e}^{\frac{24181}{T}}\right)T^3\\&+2.04941\times10^{-136}\,\mathrm{Li}_{3.0}\left(\mathrm{e}^{\frac{28378.2}{T}}\right)T^3 + 2.111387\times10^{-132}\,\mathrm{dilog}\left(1.0-1.0\mathrm{e}^{\frac{24181}{T}}\right)T^2\\&-2.90794\times10^{-132}\,\mathrm{dilog}\left(1.0-1.0\mathrm{e}^{\frac{28378.2}{T}}\right)T^2 + 1.70185\times10^{-128}\ln\left(1.0-\mathrm{e}^{\frac{24181}{T}}\right)T\\&-2.75074\times10^{-128}\ln\left(1.0-\mathrm{e}^{\frac{28378.2}{T}}\right)T + 9.227\times10^{-125}\Bigg|\Bigg) - 4.34294\ln\left(|T|\right).\end{aligned} \tag{37}$$

Figure 11 gives the $BC$ as given by the integral with polylogarithms and the observed $BC$ for the main sequence as reported in table 15.7 in [13].

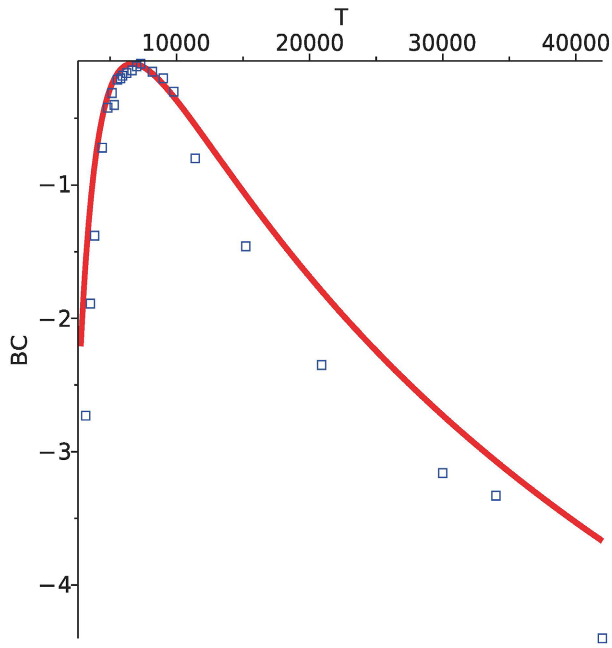


Figure 11. The bolometric correction, ($BC$), with Equation (37), red full line and observed data [13], blue squares.

The above expression for $BC$ is an analytical result but has a complicated structure. So, we now present a Taylor series of order 4 as a function of the temperature

$$\begin{aligned}BC_{app} = &\frac{\frac{5\ln(5)}{2} - 10\ln(\pi) + 74.4899 - \frac{15\ln(T)}{2}}{\ln(10)} - \frac{32988.91}{\ln(10)T}\\&-\frac{7.22474\times10^{7}}{\ln(10)T^2} + \frac{4.008268\times10^{9}}{\ln(10)T^3} + 2.30335.\end{aligned} \tag{38}$$

Figure 12 gives both the exact and the approximated $BC$s.

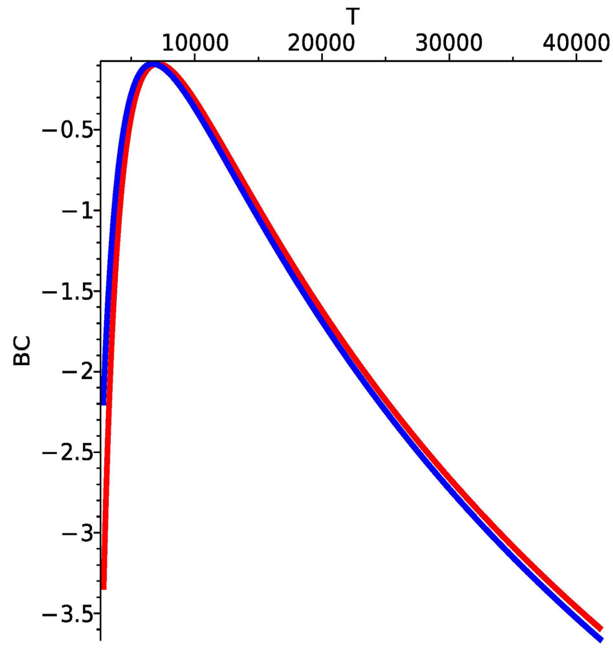


**Figure 12.** The bolometric correction, ($BC$), with Equation (37), blue full line and the approximate bolometric correction, ( $BC_{app}$ ), red full line.

## 4. Revisiting the Hertzsprung-Russell Diagram

We briefly review the formulas that characterize the visual magnitude, $M_V$ , the mass, $\mathcal{M}$, the radius, $R$ , the luminosity, $L$ , and the logarithm of the gravity, $\log(g)$, of the stars for each MK class as a function of the intrinsic, unreddened color index $(B\text{-}V)_0$, see [16] [17] for details. We start with the simplest relation between the unreddened $(B\text{-}V)_0$ and the temperature, $T$ :

$$(\text{B-V})_0 = K_{\text{BV}} + \frac{T_{\text{BV}}}{T}, \tag{39}$$

where $K_{\text{BV}}$ and $T_{\text{BV}}$ are two parameters that are derived in Equation (31a) from the least square fitting procedure. In order to continue, we invert the above relation

$$T = \frac{T_{\text{BV}}}{(\text{B-V})_0 - K_{\text{BV}}}. \tag{40}$$

The first equation models the visual magnitude, $M_V$ ,

$$\begin{aligned} M_V = & -2.5a_{\text{LM}} - 2.5b_{\text{LM}}a_{\text{MT}} - 2.5b_{\text{LM}}b_{\text{MT}} \log_{10}\left(\frac{T_{\text{BV}}}{(B-V)_0 - K_{\text{BV}}}\right) \\ & - K_{\text{BC}} + 10\log_{10}\left(\frac{T_{\text{BV}}}{(B-V)_0 - K_{\text{BV}}}\right) + \frac{T_{\text{BC}}}{T_{\text{BV}}}\left[(B-V)_0 - K_{\text{BV}}\right] + M_{\text{bol},\odot}. \end{aligned} \tag{41}$$

The second equation connects the mass of the star, $\mathcal{M}$, with $(B-V)_0$

$$\log_{10}\left(\frac{\mathcal{M}}{\mathcal{M}_\odot}\right) = a_{\text{MT}} + b_{\text{MT}} \ln\left(\frac{T_{\text{BV}}}{(\text{B-V})_0 - K_{\text{BV}}}\right)(\ln(10))^{-1}, \tag{42}$$

where $\mathcal{M}_\odot$ is the sun's mass. The third equation relates the radius, $R$ , with

(B-V)$_0$

$$\log_{10}\left(\frac{R}{R_{\odot}}\right)=1/2\,a_{\mathrm{LM}}+1/2\,b_{\mathrm{LM}}a_{\mathrm{MT}}+2\frac{\ln\left(T_{\odot}\right)}{\ln\left(10\right)}$$
$$+1/2\,b_{\mathrm{LM}}b_{\mathrm{MT}}\ln\left(\frac{T_{\mathrm{BV}}}{(\mathrm{B\text{-}V})_0-K_{\mathrm{BV}}}\right)\left(\ln\left(10\right)\right)^{-1} \tag{43}$$
$$-2\ln\left(\frac{T_{\mathrm{BV}}}{(\mathrm{B\text{-}V})_0-K_{\mathrm{BV}}}\right)\left(\ln\left(10\right)\right)^{-1},$$

where $R_{\odot}$ is the sun's radius. The fourth equation connects the luminosity of a star, $L$, with (B-V)$_0$

$$\log_{10}\left(\frac{L}{L_{\odot}}\right)=a_{\mathrm{LM}}+b_{\mathrm{LM}}a_{\mathrm{MT}}+b_{\mathrm{LM}}\left(b_{\mathrm{MT}}\ln\left(\frac{T_{\mathrm{BV}}}{(\mathrm{B\text{-}V})_0-K_{\mathrm{BV}}}\right)\frac{1}{\ln\left(10\right)}\right), \tag{44}$$

where $L_{\odot}$ is the sun's luminosity.

A fifth fundamental parameter is the surface gravity, $g$, which is defined as

$$g=G\frac{M}{r^2}, \tag{45}$$

where $M$ is the mass of the body, $r$ its radius, $G$ is the Newtonian gravitational constant which has the value $G=6.6742\times10^{-11}\frac{\mathrm{m}^3}{\mathrm{kg}\cdot\mathrm{s}^2}$, [18], $R_{sun}=6.95508\times10^{8}\ \mathrm{m}$ and $M_{sun}=1.989\times10^{30}\ \mathrm{kg}$, see [13]. We now find the logarithm of the surface gravity as a function of (B-V)$_0$

$$\log\left(g\left[\mathrm{cgs}\right]\right)=-10.60+0.4342$$
$$\times\ln\left(\mathrm{e}^{2.302a_{\mathrm{MT}}-2.302a_{\mathrm{LM}}-2.302b_{\mathrm{LM}}a_{\mathrm{MT}}}\left(\frac{T_{\mathrm{BV}}}{(\mathrm{B\text{-}V})_0-K_{\mathrm{BV}}}\right)^{b_{\mathrm{MT}}-b_{\mathrm{LM}}b_{\mathrm{MT}}+4}\right), \tag{46}$$

or as a function of the temperature

$$\log\left(g\left[\mathrm{cgs}\right]\right)=\frac{10.2198}{\ln\left(2\right)+\ln\left(5\right)}+\frac{\ln\left(10^{a_{\mathrm{MT}}+\frac{b_{\mathrm{MT}}\ln\left(T\right)}{\ln\left(2\right)+\ln\left(5\right)}}\right)}{\ln\left(2\right)+\ln\left(5\right)}$$
$$-\frac{2\ln\left(10^{\frac{a_{\mathrm{MT}}b_{\mathrm{ML}}\ln\left(5\right)+a_{\mathrm{MT}}b_{\mathrm{ML}}\ln\left(2\right)+b_{\mathrm{ML}}b_{\mathrm{MT}}\ln\left(T\right)+a_{\mathrm{ML}}\ln\left(5\right)+a_{\mathrm{ML}}\ln\left(2\right)+4\ln\left(T_{sun}\right)-4\ln\left(T\right)}{2\ln\left(2\right)+2\ln\left(5\right)}}\right)}{\ln\left(2\right)+\ln\left(5\right)}. \tag{47}$$

The first six parameters of the eight which characterize the theory for the HR diagram here adopted are given in **Table 2**.

The other two parameters are given in **Table 3** together with the two values obtained by processing the observational data reported in [5].

**Figure 13** gives the theoretical and the observed $M_V$ as functions of the color (B-V); theoretical data as in **Tables 2-3**, observed $M_V$ as in [5].

**Table 2.** Table of first six coefficients here used.

| | MAIN, V |
|---|---|
| $K_{BV}$ | −0.5366479 |
| $T_{BV}[K]$ | 6326.41833 |
| $K_{BC}$ | 43.0292691 |
| $T_{BC}[K]$ | 31771.2971 |
| $a_{LM}$ | $6.2091146 \times 10^{-2}$ |
| $b_{LM}$ | 3.436079 |

**Table 3.** Table of $a_{MT}$ and $b_{MT}$ in two cases.

| | this paper | paper [5] |
|---|---|---|
| $a_{MT}$ | −7.66 | −6.29 |
| $b_{MT}$ | 2.01 | 1.67 |

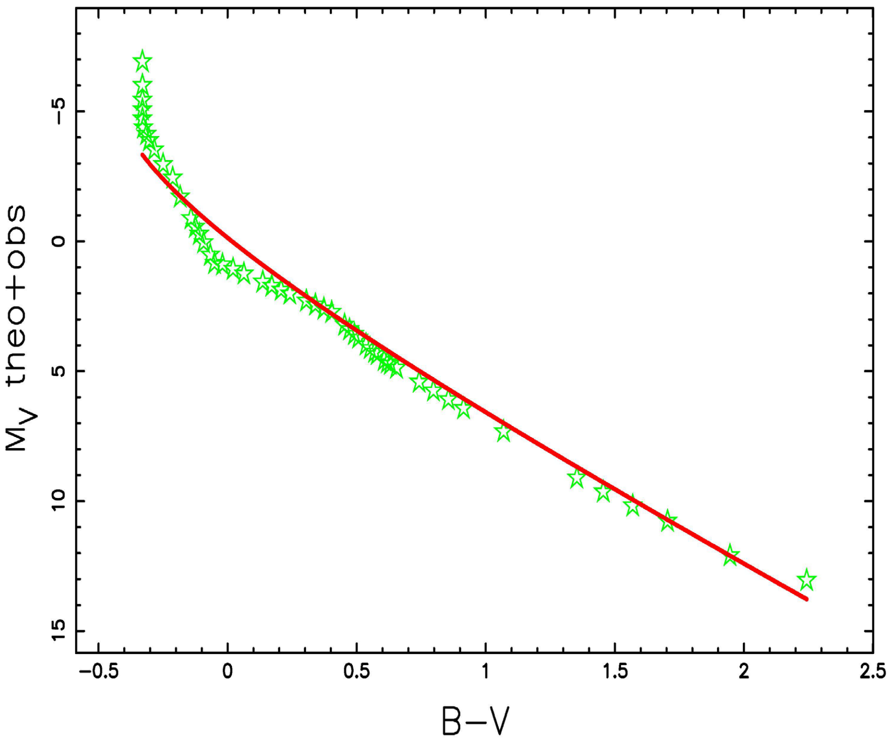


**Figure 13.** Theoretical $M_V$ versus (B-V), red line, and observed data [5], green stars, of nearby main sequence stars.

The radii, the masses and the luminosities are presented in **Figures 14-15** and 16 as functions of (B-V).

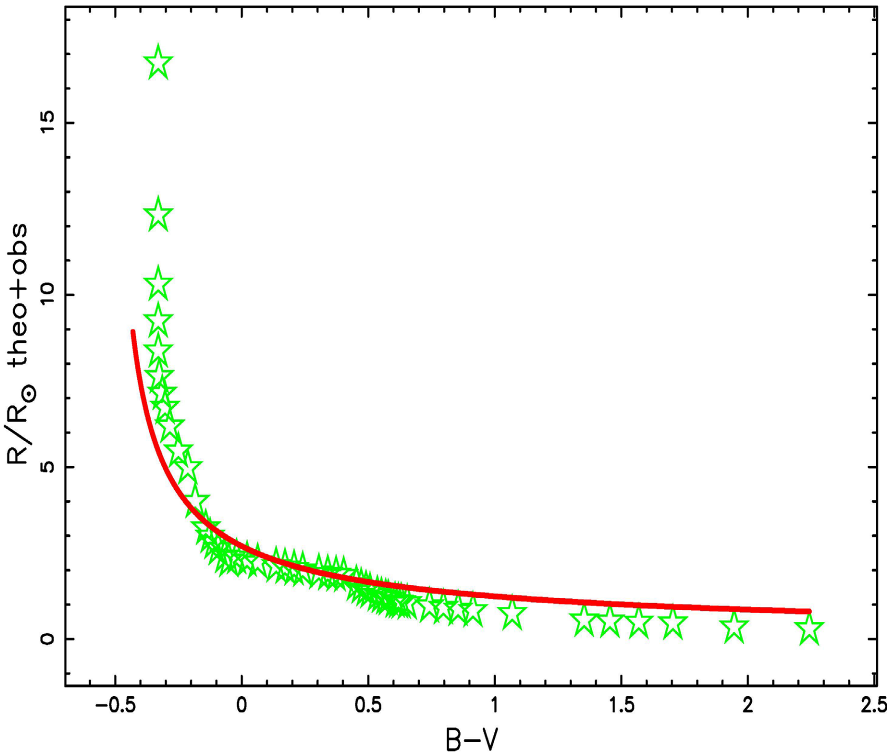


**Figure 14.** Theoretical radius versus (B-V), red line, and observed data [5], green stars, of nearby main sequence stars.

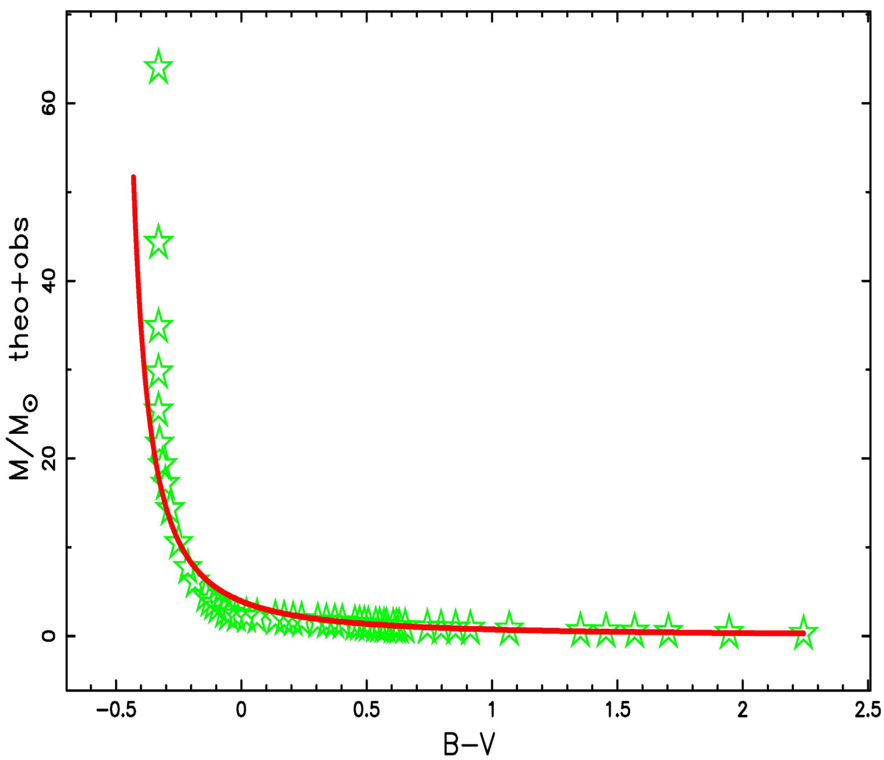


**Figure 15.** Theoretical mass versus (B-V), red line, and observed data [5], green stars, of nearby main sequence stars.

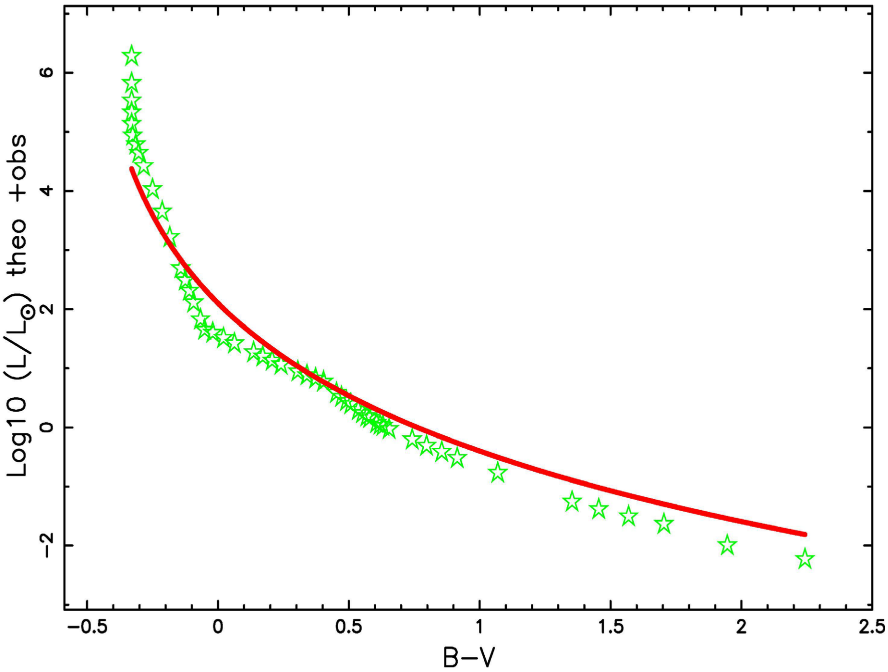


**Figure 16.** Logarithm base 10 of theoretical luminosity versus (B-V), red line, and observed data [5], green stars, for nearby main sequence stars.

**Figure 17** presents $\log(g)$ as a function of the temperature.

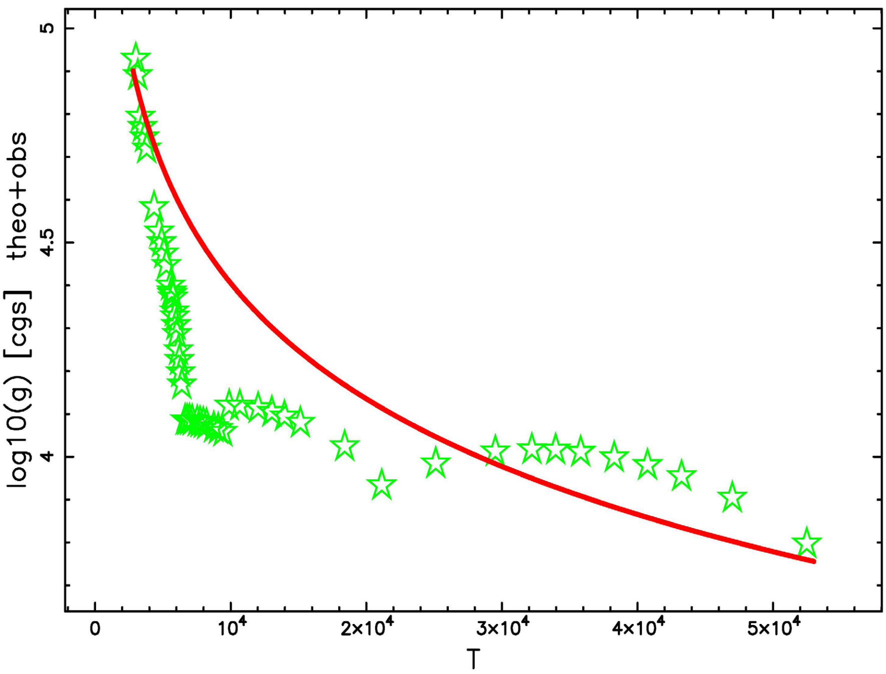


**Figure 17.** Theoretical $\log_{10}(g)$ in cgs versus (B-V), red line, and observed data [5], green stars, of nearby main sequence stars.

## 5. Conclusions

**Polylogarithms:** The asymptotic expansions for the three polylogarithms $\mathrm{Li}_2$,

$\mathrm{Li}_3$ and $\mathrm{Li}_4$ were derived, see Equations (22)-(24). The incomplete Planck distribution in wavelengths was integrated in terms of the polylogarithms, see Equation (25).

**Astronomical colors:** The color (B-V) as given by the incomplete Planck integral versus temperature was given in Figure 6 for the main sequence stars. In order to reproduce some common astronomical results, (B-V) and (U-B) were found as functions of $1/T$, see Figures 7-8.

**Bolometric correction:** The bolometric correction evaluated in terms of polylogarithms as a function of the temperature was presented in Figure 11 and Figure 12 presents a Taylor approximation.

**HR diagram:** We have updated the eight-parameter model of [16] [17] by inserting four parameters derived from the color theory with polylogarithms. In particular, we modeled the visual magnitude, see Figure 13, the mass, see Figure 15 the radius, see Figure 14, the logarithm of the luminosity, see Figure 16 and the logarithm of the gravity, see Figure 17, of nearby main sequence stars.

**Future work:** Here we have applied the color theory with polylogarithms to the MS stars. The following categories of stars still wait to be analyzed: white dwarfs, giants III, super-giants and B0-B5 super-giants.

## Conflicts of Interest

The author declares no conflicts of interest regarding the publication of this paper.

## References


[1] Lewin, L. (1981) Polylogarithms and Associated Functions. North Holland.

[2] Clark, B.A. (1987) Computing Multigroup Radiation Integrals Using Polylogarithm-Based Methods. *Journal of Computational Physics*, **70**, 311-329. https://doi.org/10.1016/0021-9991(87)90185-9

[3] Lampret, V., Peternelj, J. and Krainer, A. (2002) Luminous Flux and Luminous Efficacy of Black-Body Radiation: An Analytical Approximation. *Solar Energy*, **73**, 319-326. https://doi.org/10.1016/s0038-092x(02)00119-6

[4] Condon, J.J. and Ransom, S.M. (2016) Essential Radio Astronomy. Princeton University Press.

[5] Eker, Z., Soydugan, F., Bilir, S., Bakış, V., Aliçavuş, F., Özer, S., *et al.* (2020) Empirical Bolometric Correction Coefficients for Nearby Main-Sequence Stars in the *Gaia* Era. *Monthly Notices of the Royal Astronomical Society*, **496**, 3887-3905. https://doi.org/10.1093/mnras/staa1659

[6] Roughan, M. (2020) The Polylogarithm Function in Julia. arXiv:2010.09860.

[7] Voigt, A. (2022) Comparison of Methods for the Calculation of the Real Dilogarithm Regarding Instruction-Level Parallelism. arXiv:2201.01678.

[8] Delgado-Bonal, A. (2017) Entropy of Radiation: The Unseen Side of Light. *Scientific Reports*, **7**, Article No. 1642. https://doi.org/10.1038/s41598-017-01622-6

[9] Lewis, W. and McClarren, R.G. (2025) Fast, Accurate Numerical Evaluation of Incomplete Planck Integrals. *Annals of Nuclear Energy*, **218**, Article 111374. https://doi.org/10.1016/j.anucene.2025.111374

[10] Sekiguchi, M. and Fukugita, M. (2000) A Study of the *B*-*V* Color-Temperature Rela-

tion. *The Astronomical Journal*, **120**, 1072-1084. https://doi.org/10.1086/301490

[11] Ballesteros, F.J. (2012) New Insights into Black Bodies. *EPL (Europhysics Letters)*, **97**, Article 34008. https://doi.org/10.1209/0295-5075/97/34008

[12] Kraus, J.D. (1986) Radio Astronomy. Cygnus-Quasar Books.

[13] Cox, A.N. (2000) Allen's Astrophysical Quantities. Springer.

[14] Olver, F.W.J., Lozier, D.W., Boisvert, R.F. and Clark, C.W. (2010) NIST Handbook of Mathematical Functions. Cambridge University Press.

[15] Olson, T. (1998) The Colors of the Stars. *Color and Imaging Conference*, **6**, 233-240. https://doi.org/10.2352/cic.1998.6.1.art00050

[16] Zaninetti, L. (2008) Semi-Analytical Formulas for the Hertzsprung-Russell Diagram. *Serbian Astronomical Journal*, **177**, 73-85. https://doi.org/10.2298/saj0877073z

[17] Zaninetti, L. (2009) Semi-Analytical Formulas for the Fundamental Parameters of Galactic Early B Supergiants. *Serbian Astronomical Journal*, **179**, 69-74. https://doi.org/10.2298/saj0979069z

[18] Mohr, P.J. and Taylor, B.N. (2005) CODATA Recommended Values of the Fundamental Physical Constants: 2002. *Reviews of Modern Physics*, **77**, 1-107. https://doi.org/10.1103/revmodphys.77.1